

1 **The NCAS Mobile Dual-Polarisation Doppler X-Band Weather**

2 **Radar (NXPol)**

3 Ryan R. Neely III^{1,2}, Lindsay Bennett^{1,2}, Alan Blyth^{1,2}, Chris Collier^{1,2}, David Dufton^{1,2}, James
4 Groves^{1,2}, Daniel Walker^{1,2}, Chris Walden^{1,3,4}, John Bradford^{1,3,4}, Barbara Brooks^{1,2}, Freya Addison^{1,2},
5 John Nicol¹, Ben Pickering^{1,2}

6
7 ¹National Centre for Atmospheric Science, University of Leeds, Leeds, UK

8 ²School of Earth and Environment, University of Leeds, Leeds, UK

9 ³Rutherford Appleton Laboratory, Didcot, UK

10 ⁴National Facility for Atmospheric and Radio Research (NFARR), Chilbolton, Hampshire, UK

11

12 *Correspondence to:* Ryan R. Neely III (r.neely@ncas.ac.uk)

13 **Abstract.** In recent years, dual-polarisation Doppler X-band radars have become a widely used part of the atmospheric
14 scientist's toolkit for examining cloud dynamics and microphysics and making quantitative precipitation estimates. This is
15 especially true for research questions that require mobile radars. Here we describe the National Centre for Atmospheric
16 Science (NCAS) mobile X-band Dual-polarisation Doppler weather radar (NXPol) and the infrastructure used to deploy the
17 radar and provide an overview of the technical specifications. It is the first radar of its kind in the United Kingdom. The
18 NXPol is a Meteor 50DX manufactured by Selex-Gematronik (Selex ES GmbH), modified to operate with a larger 2.4 m
19 diameter antenna that produces a 0.98° half-power beam width and without a radome. We provide an overview of the
20 technical specifications of the NXPol with emphasis given to the description of the aspects of the infrastructure developed to
21 deploy the radar as an autonomous observing facility in remote locations. To demonstrate the radar's capabilities, we also
22 present examples of its use in three recent field campaigns and its ongoing observations at the National Facility for
23 Atmospheric and Radio Research (NFARR).

24

25 **1 Introduction**

26 Polarimetric radars are powerful tools for meteorological studies. The diverse quantities observed by polarimetric radars can
27 provide significant insights into the evolution of clouds and precipitation (e.g. Fabry, 2015). Thus, small and or mobile dual-
28 polarisation Doppler X-band radars have become popular tools for examining cloud microphysics and dynamics as well as
29 making quantitative precipitation estimates (QPE) in mobile applications (Wurman et al. 1997; Matrosov et al. 2005; Wang
30 and Chandrasekar, 2010). Currently, a significant number of such radars exist in the operational and research sectors to
31 address a broad range of scientific goals pertaining to atmospheric physics and hydrometeorology (Maki et al. 2005;
32 Bluestein et al. 2007; 2014; Kato, A. and Maki, 2009; Pazamny et al. 2013; Forget et al. 2016; Mishra et al. 2016; Antonini
33 et al. 2017). Use of such radars notably includes recent field campaigns such as PECAN (Plains Elevated Convection At
34 Night, Geerts et al., 2016), where a variety of mobile radars (both X-band and C-band) from multiple institutions were used
35 collaboratively to achieve complex goals successfully. In the United States, where mobile research radars are more
36 numerous, large multi-institution observational campaigns, similar to PECAN, occur several times a decade (e.g. the second
37 Verification of the Origins of Rotation in Tornadoes Experiment (VORTEX-2), Wurman et al. (2012)). Mobile radars are
38 also used as a teaching resource, for example, the University of Oklahoma SMART (Shared Mobile Atmospheric Research
39 and Teaching) radar (Biggerstaff et al., 2005). Thus, it is difficult to understate the role of such instrumentation in
40 hydrometeorology and atmospheric research.

41
42 Here we describe the NCAS Mobile X-band dual-polarisation Doppler weather radar (NXPol) shown in Figure 1 and the
43 supporting infrastructure structure that has been developed to support the radar when on deployment. The NXPol is the first
44 dual-polarisation mobile radar in the United Kingdom. The supporting infrastructure has been developed to create a robust
45 facility that may be operated remotely with minimal staff. As such, the NXPol has developed into a semi-operational
46 observing system facility that has the significant capabilities present in both traditional research radars used for intensive
47 operational periods (IOPs) and radars operated as part of national networks. In addition to the technical description,
48 examples of NXPol in 3 differing campaigns are shown, as well as an example of its ongoing use at the National Facility for
49 Atmospheric Radar Research (NFARR) located at the Chilbolton Observatory. The NXPol is part of the pool of mobile
50 instruments that make up the UK NCAS Atmospheric Measurement Facility (NCAS-AMF),

51 <https://www.ncas.ac.uk/index.php/en/about-amf>) so it is available for use by the community according to the procedures set
52 out by NCAS-AMF.

53 **Figure 1: Photograph of the NXPoI collecting data at Burn Airfield near Selby, UK. Here the NXPoI is deployed using only its
54 trailer as a platform.**



55

56 **2 Technical Summary of the NXPol**

57 The NXPol is a modified mobile Meteor 50DX (Selex ES GmbH) X-band, dual-polarisation, Doppler weather radar. The
58 radar is a magnetron based system and operates at a nominal frequency of 9.375 GHz (~3.2 cm). A detailed description of
59 the development of this class of Selex radars is given by Borgmann et al. (2007). The radar is capable of measuring areal
60 precipitation, radial winds and properties of cloud and precipitation particles. It can also detect non-meteorological echoes,
61 including biota, at close range by scanning at slower speeds and optimising the transmitter and receiver. Similar radars
62 (including the newer Meteor 60DX) are utilised by national weather services and research centres throughout the world.
63 Table 1 provides a summary of the technical characteristics of the NXPol.

64
65 Like all standard mobile Meteor 50/60DX radars, NXPol is transportable. The radar is constructed on a wheeled platform
66 that is approved for towing on roads in the European Union by a 4x4 vehicle and can also be lifted by a crane. This trailer
67 includes a generator to provide necessary power and the communications infrastructure to operate and monitor the radar
68 remotely for up to 24 hours. This mobility makes NXPol a highly versatile tool for studying a diverse array of atmospheric
69 phenomenon across the globe. The main difference between NXPol and the standard mobile Meteor 50/60DX is that the
70 NXPol has been fitted with a larger 2.4 m diameter antenna that produces a 0.98° half-power beam width. The NXPol is
71 operated without a radome, which is beneficial for eliminating radome attenuation effects, but extra care is required during
72 transport, and long-distance shipping may need the antenna and external waveguides to be removed. The decision to fit
73 NXPol with a larger antenna was made to support the ability to make higher resolution observations of convective clouds.
74 In comparison, the standard mobile Meteor 50/60DX has a 1.8m antenna that produces a 1.3° half-power beam width and is
75 usually operated with a radome. In addition to its increased spatial resolution, NXPol is also advantageous for use in the
76 observation of cloud evolution because of its rapid scanning capabilities; up to 36 degs^{-1} .

77 **Table 1. Technical characteristics of the NXPol.**

Parameter	Specifications
Frequency	9.375 GHz
Transmitter Type	Coaxial Magnetron
Pre-Split Peak Transmit Power	~75 kW (half to each channel)
Average Power	~80W
Dual-Polarisation Mode	Simultaneous H & V
Digital Receiver and Signal Processor	GDRX®4
Receiver Linearity	90 dB +/- 0.5 dB
Antenna Diameter	2.4m
Half Power Antenna Beam Width	0.98°
Antenna Gain	44dB
Minimum Discernible Signal (2µs pulse)	H: -118dBm V: -117dBm
Sensitivity (2µs pulse at 100km)	~-11dBZ
Radome	None
Elevation Scan Range	-1 to 181°
Azimuthal Scan Range	0 to 360°
Position Accuracy	±0.1°

78 **2.1 Operations**

79 The NXPol can be operated via a remote computer (e.g. a laptop or server) that connects by wireless, ethernet or 3G to PCs
80 onboard the NXPol's trailer unit. The operational software allows the user to set up the radar for deployment and schedule
81 the scanning sequence. [Ravis®](#) is the maintenance and calibration software used for system diagnostics and testing, as well
82 as real-time data visualisation. Ravis® includes an automatic sun tracking tool for alignment of the system. [Rainbow®5](#) is
83 the scan scheduling, data visualisation and analysis software, providing near real-time product and image generation. As
84 shown in Table 2, the NXPol is highly configurable with regards to the pulse width, PRF and scan pattern and can be tailored
85 to address the specific scientific question being examined. Bold values in Table 2 indicate the typical parameter settings used
86 in the examples shown in Section 3. Signal retrieval, analysis and data storage are performed by the [GDRX®4](#) digital
87 receiver and signal processor.

88

89

90 **Table 2. Parameter settings. Boldface indicates settings typically used for operations.**

Parameter	Specifications
Pulse Width	0.5 μ s, 1 μ s, 2 μ s (1μs)
Pulse Repetition Frequency (PRF; Single or Dual Modes)	250-2000 Hz (1000 Hz single-PRF mode, 1000Hz/800Hz dual-PRF mode)
Dual PRF Mode	3/2, 4/3, 5/4 (5/4)
Unambiguous Velocity using single-PRF	± 8 m/s - ± 16 m/s (± 8m/s)
Unambiguous Velocity using dual-PRF	± 8 m/s - ± 64 m/s (± 32m/s)
Range Resolution	50m-300m (150m)
Maximum Range Gates	2000 (2000)
Maximum Operating Range	600 km (150 km)
Antenna Speeds	0 to 36 $^{\circ}$ s $^{-1}$ (~ 13-24° s$^{-1}$)

91

92 Note that the NXPol operates only using the hybrid polarisation basis, also known as the simultaneous transmit and receive
93 (STAR) mode (i.e. it splits the transmitted signal into two parts and simultaneously transmits and receives horizontal (H) and
94 vertical (V) polarisations) (Chandrasekar and Bharadwaj, 2009). This mode operates under the assumption that the cross-
95 polarisation signals are weak in comparison to the co-polar signals and are therefore negligible (Wang and Chandrasekar,
96 2006)). As the cross-polar signals are not measured, observations of the linear depolarisation ratio (LDR) are not available.
97 The benefit of STAR mode is that the NXPol has a much simpler and robust hardware design because it avoids switching
98 between H and V polarisation on a pulse-to-pulse basis (Doviak et al. 2000; Bringi and Chandrasekar 2001). STAR mode
99 operations also lead to less noisy measurements of differential reflectivity (Z_{DR}) and other quantities while operating at rapid
00 scan speeds.

01 The dual-polarisation capability of the NXPol allows for the retrieval of many additional geophysically-related variables.
02 This additional information helps to provide insight into the size and shape of precipitation, enhanced target identification as
03 well as the assessment of attenuation and propagation effects (Bringi and Chandrasekar, 2001; Kumjian 2013a;b;c; Fabry,
04 2015). The NXPol's polarimetric ability also enables many alternative methods for quantitative precipitation estimation,
05 which are demonstrated in Section 3 (Deiderich et al. 2015; 2015). In addition to the standard polarimetric variables

06 provided by most operational dual-polarisation radars, NXPol also provides the of the degree of polarisation (DOP) of the
07 backscattered signal. DOP is a relatively unexplored variable with respect to atmospheric phenomenon, but previous
08 examinations have shown that it has similar properties as the co-polar correlation coefficient when classifying hydrometeors
09 (Galletti et al. 2007; 2012). Galletti et al. (2012) note that DOP is advantageous compared to the co-polar correlation
10 coefficient for STAR mode radars like the NXPol because it retains its physical meaning even when observing scatterers that
11 are cross polarising (i.e. with linear depolarisations ratios that are greater than zero).

12

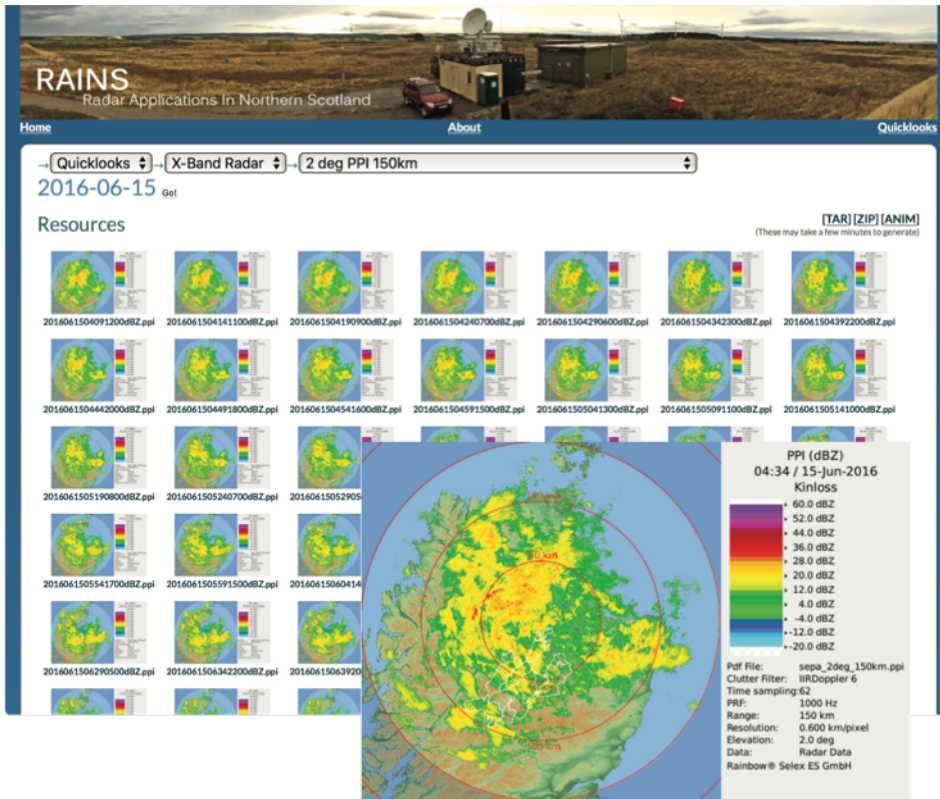
13 During operations, scan strategies are tailored to the application but typically sample a volume out to 150 km in range every
14 5 minutes. The typical volume includes ~10 PPI scans between 0.5° and 30° of elevation and a calibration scan at 90°. All
15 data are recorded as moments in Selex's Rainbow®5 format (a flavour of XML). This format is easily utilised by common
16 open-source analysis software packages (Heistermann et al. 2015) such as the LIDAR RADAR Open Software Environment
17 (LROSE) that is provided by the Earth Observing Laboratory within the U.S.'s National Center for Atmospheric Research
18 (NCAR) (Dixon et al. 2012; 2013), the Python Atmospheric Measurement Radiation (ARM) Climate Research Facility
19 Radar Toolkit (PyART) (Helmus and Collis, 2016) and the Open Source Library for Weather Radar Data Processing
20 (wradlib) (Heistermann et al. 2013). The NXPol has the capability of collecting raw IQ data for post-processing, but this is
21 typically not done due to the size of the dataset.

22

23 Once a volume is collected, the raw data are backed up locally and transferred to a central NCAS data storage facility if
24 internet capacity allows as described in Section 2.2. In addition to storing the data for later analysis, Rainbow®5 generates
25 several quick-look images in real-time (tailored to the application of the radar). The quick-look images are transferred to a
26 central server where they are uploaded onto a web catalogue to disseminate the observations in near real-time and enable
27 easy examination of past observations. Figure 2 depicts an example of a real-time image and corresponding catalogue page.
28 Such near-real-time quick-look charts were crucial in the two field campaigns discussed later for changing scan patterns and
29 directing aircraft. The quick-look images were also helpful to the NXPol's operators and forecasters at the Scottish
30 Environmental Protection Agency and the U.K.'s Met Office during the six-month-long Radar Applications in Northern
31 Scotland (RAINS) campaign in 2016 (Section 3.3) for assessing the impact that a radar in this location would have on
32 observational quality in near-real-time conditions in comparison to existing observations.

33

34 Figure 2. Example of the data catalogue used to monitor the NXPoI observations in near-real time during the RAINS project
35 described in Section 3.3. The background shows a collection of a set of images from a single day while the foreground highlights an
36 example of a near-real-time image produced by Rainbow®5.



37

38 2.2 Deployment Setup

39 The operational requirements dictated by the strategic and project-specific scientific goals of the NXPol have led to the
40 development of bespoke infrastructure to support the radar during operations. The primary requirements for deploying the
41 NXPol radar are visibility, security, power and internet access. Considering these options, the NXPol may be deployed using
42 solely its integrated trailer (as in Figure 1) or in conjunction with a platform structure as depicted in Figure 3. The platform
43 setup is based on a similar scheme employed by Selex ES GmbH for the NXPol's deployment during the Single European
44 Sky ATM (Air Traffic Management) Research (SESAR) campaign in 2015 at Braunschweig Airport near Hanover,
45 Germany. The setup has the major advantage of lifting the radar off the ground to provide greater visibility. It also makes
46 security and public safety issues (See Section 2.3) less problematic.

47
48 The platform consists of a 20-foot standard shipping container and a 20-foot office container set side by side along their long
49 axis. To provide the necessary structural strength to support the weight of the NXPol, on top of each of the containers is a
50 20-foot platform container (also known as a 'flat rack'). Using standard shipping containers and platforms dramatically
51 reduces engineering time and cost during deployments. Also, because of their global ubiquitousness, the elements needed to
52 construct a similar platform can be sourced locally. This further reduces deployment costs. To provide safe access to the
53 radar while it is on the platform, a staircase and railing are constructed from standard scaffolding materials as shown in
54 Figure 3. Also attached to the platform structure are the various pieces of hardware that support a long-term autonomous
55 deployment of the NXPol; lightning protection, a satellite internet connection, security camera and local weather station.

56
57 In addition to providing a platform for the NXPol, the office unit provides space for the additional IT infrastructure needed
58 for NXPol's autonomous operation (described below). The office also provides a base of operations for staff while on site
59 during remote fieldwork. The office is particularly useful during observational campaigns that involve the coordinated
60 operation of the radar and an aircraft (such as the ICE-D campaign described in Section 3.2). During such campaigns, staff
61 can monitor and direct the radar's observations in real-time and communicate with the aircraft to help target the
62 observations.

63 **Figure 3. NXPoI deployed at Chilbolton Observatory, Hampshire, UK. Seen in the picture is the 20' shipping container, 20' office**
64 **container, two 20' platform containers and scaffolding used to construct a platform for the radar.**



65
66

67 There is also the need in the scientific community for the collection of statistically meaningful observations over a wide
68 range of synoptic conditions. This requirement has necessitated the move to semi-permanent, continuous and autonomous
69 operations that last for many months. The RAINS project and on-going work at NFARR (where the NXPoI will operate for
70 several months at a time between campaign deployments) in particular demonstrate the need for this type of facility to
71 support the radar in its long-term operations.

72

73 Table 3 summarises the operational requirements of the NXPoI. Data and power availability vary depending on the
74 deployment. Typically, when the NXPoI is deployed for less than 24 hours, the onboard generator supplied by an 80 L fuel
75 tank provides all electricity. An onboard 3G mobile data connection or satellite link provide internet connectivity. When the
76 NXPoI is deployed using the container platform, mains electricity is connected to the radar's electrical grid and the onboard
77 generator acts as a backup power supply that is automatically started upon loss of mains power. Additionally, the 3G mobile

78 data connection is supplemented with a local area network connection or a satellite internet connection. This allows for
79 more robust autonomous and remote operation of the system.

80

81 **Table 3. Operational conditions and logistical requirements of the NXPol.**

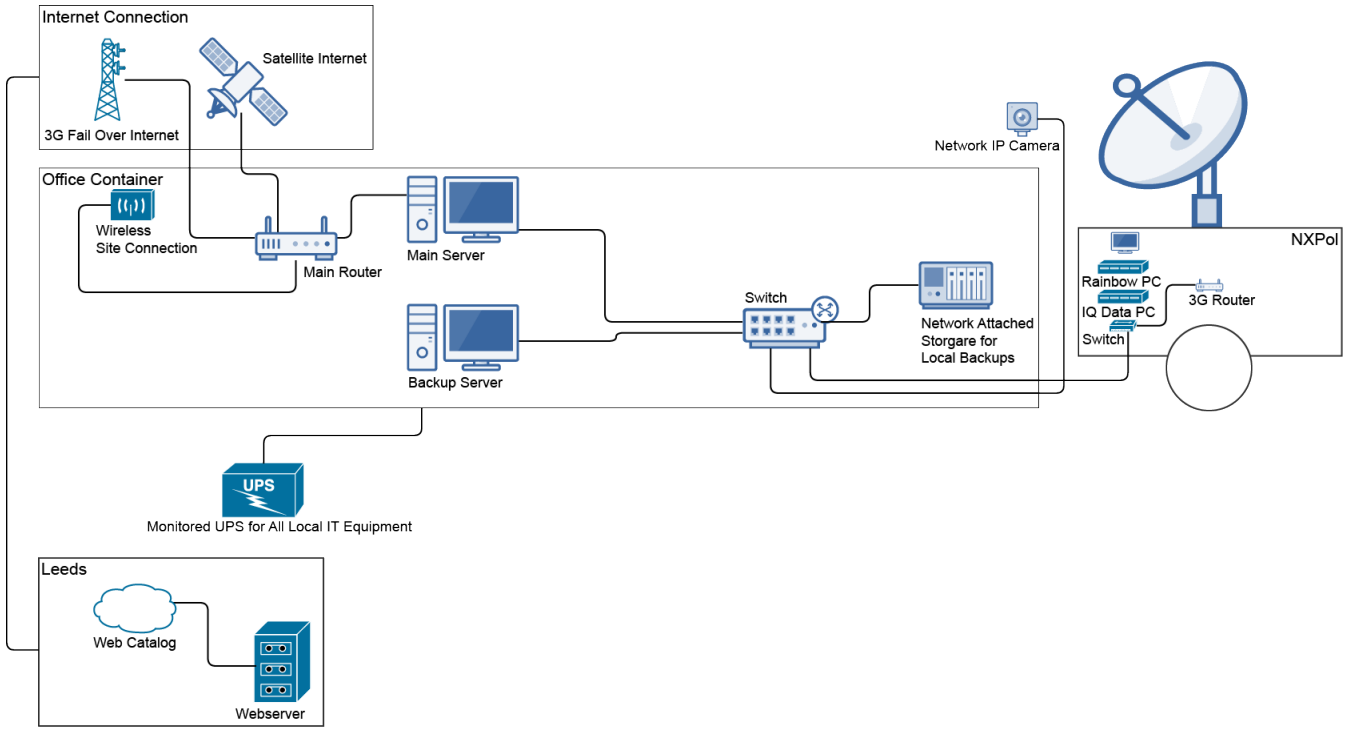
Conditions	Specifications
Max Operational Wind Speed without Radome	56 mph (90km/h)
Electrical Supply	3-phase 32A Service or Onboard Diesel Generator
Power Consumption	8kW (average), 12kW (max)
Operating Temperatures	-10C to 35C
Total Weight, Nose weight	2800kg, 120kg
Width (without supports, with supports)	2.550m, 3.560m
Height (0 degs, 90 degs)	3.995m, 4.250m
Max drive Speed	50mph (80km/h)

82

83 The IT infrastructure needed for the NXPol's autonomous operation includes a server that provides a gateway for
84 communicating with the radar and data backup. Figure 4 summarises the IT strategy. In addition to communications, the
85 infrastructure includes a local weather station to primarily monitor wind speeds, a video camera to monitor the radar's
86 movement and an Uninterruptible Power Supply (UPS) for the server. Data production is on the order of between 5 and 9 Gb
87 per day. During long-term remote operations the data can be backed-up using a commercial satellite internet system if
88 available, although it may be cost-prohibitive if there is not an unmetered period (typically in the early hours of the morning
89 local time). The onboard 3G connection provides redundancy and/or remote control, if local signal strength permits, but it is
90 not practical to backup bulk data via this route. If near-real-time remote raw data access is required, a suitable Internet
91 connection is necessary. Quick-look charts as shown in Figure 2 use considerably less data and are therefore logistically
92 simpler, potentially allowing selective download of raw data over a lower-bandwidth connection. Data are backed-up locally
93 to a Network Attached Storage (NAS) system in the office container in medium- to long-term deployments.

94

95 **Figure 4. Schematic of the IT infrastructure used by the NXPol when on deployment.**



96

97 **2.3 Safety**

98 An important consideration when deploying the NXPol radar is the protection of both operators and the public from
99 exposure to transmissions. The location of the deployment site is determined in conjunction with the required safety distance
100 specified by a radiation exposure assessment. The International Commission on Non-Ionizing Radiation Protection
101 (INCIRP) specifies that the maximum continuous exposure to radiation at frequencies between 2 GHz and 300 GHz should
102 not exceed 10Wm^{-2} in areas where the general population has access and 50Wm^{-2} for occupational exposure, averaged over
103 a period of 6 minutes (Ahlbom et al. 1998). When deployed on the ground, a safety barrier must be constructed or measures
104 put in place to prevent access within the distance which the exposure threshold would be exceeded as determined by the
105 radiation assessment (e.g. if the radar dish stops scanning). When NXPol is situated on a platform and is scanning and
106 operating as scheduled, there is no risk to people (including those with implanted medical devices) on the ground 15m from
107 the radar and, hence, this is another benefit of this method of deployment. If the radar is unmanned on the platform, then
108 access must be restricted to the distance at which public exposure limits ($10\text{W}/\text{m}^2$) are reached in the event the NXPol
109 malfunctions and stops scanning but continues to transmit.

110
111

112 The second major safety consideration is the operation of the system in high winds. Without a radome the maximum
113 operational wind speed is 56mph. The weather station continuously monitors the wind speed and notifies operators via text
114 and email alerts when a set threshold (typically below the 56mph maximum limit to allow for gusts) is exceeded. Operators
115 closely monitor the conditions during forecasted events and, in the case of significant winds, interrupt the scan schedule to
116 move the antenna into the vertical position (which provides the least wind resistance) and activate the locking stow pin to
117 prevent movement. In addition to winds, NXPol's temperature must be monitored carefully to avoid operations below -10C
118 and above 35C as there is no radome to provide a conditioned environment for the transmitter and receiver equipment boxes
119 located behind the antenna. This operational range also limits the regions where the NXPol may be deployed.

120

21 3 Example Deployments and Observations

22 Below, four examples of the use of NXPOL are given. Descriptions are provided to highlight the utilisation of the radar to
23 achieve the scientific aims of each project.

24 3.1 COPE

25 NXPOL was utilised for the first time in the CONvective Precipitation Experiment (COPE) held in the vicinity of Davidstow,
26 Cornwall during July and August, 2013. Three aircraft, including the Facility for Airborne Atmospheric Measurement
27 (FAAM) BAe-146 aircraft, and other ground-based instruments were also deployed; see Leon et al., (2015). The principal
28 aim of the project was to understand the physical processes involved in the production of heavy convective precipitation that
29 could result in flash flooding. Ultimately, predictions of heavy precipitation and potential flash floods by Numerical Weather
30 Prediction (NWP) models will be improved as a result of the new knowledge and understanding of physical processes.

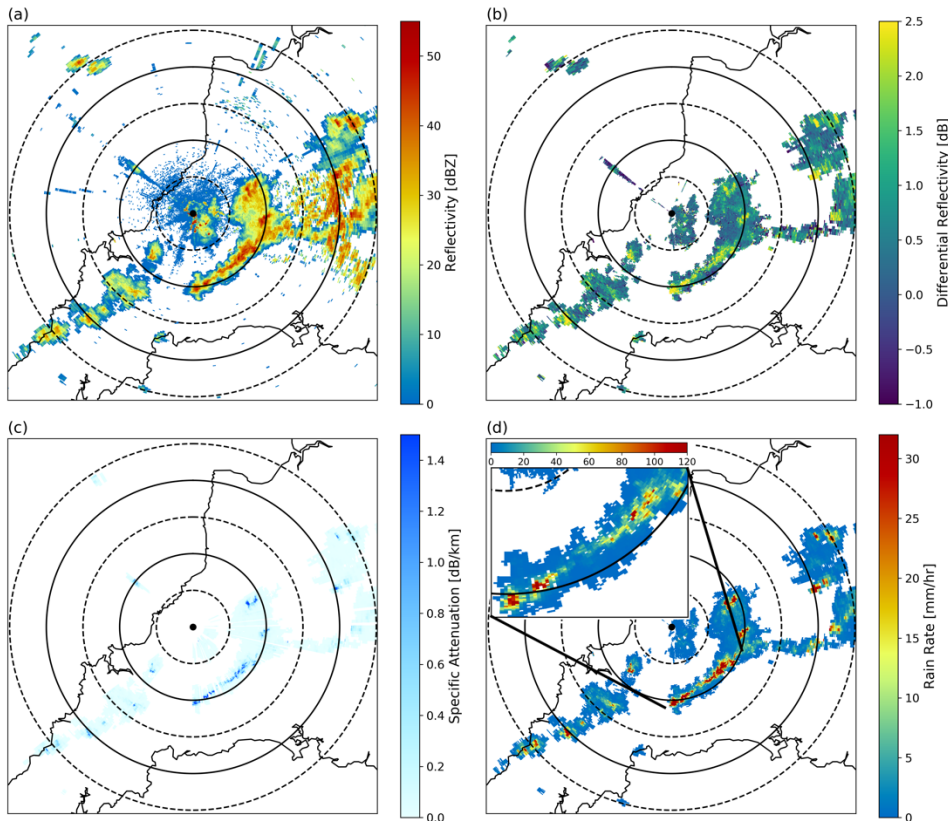
31 Several flash flooding events have previously occurred in the region, the most notable in recent years being the Boscastle
32 flood of 2004 (Golding et al. 2005). The role of the radar was to determine (a) the altitude of the first echoes; (b) the rate of
33 development of the reflectivity echoes; (c) the spatial and temporal distribution of the main echoes; (d) the particle types
34 from dual-polarisation parameters (e.g. warm rain or graupel), and (e) the maximum intensity of the precipitation.

35
36 NXPOL collected data during 16 IOPs covering a variety of synoptic and microphysical conditions including heavy
37 precipitation from shallow clouds (warm rain only) and several cases of deep convection along semi-organised convective
38 lines with similarities to the Boscastle event. An example of the convective clouds that formed along a convergence line (at
39 20 km range between S and SE) and observed elsewhere on 3 August, 2013 is shown in Figure 5. Note that Figure 5 and all
40 following figures were created using software developed in NCAS that is based on the Py-ART software suite (Helmus and
41 Colis, 2016). The rainfall rates (Figure 5d) were derived from the unfiltered and uncorrected calibrated horizontal
42 reflectivity (Z_H , Figure 5a) by first applying a second trip filter and a fuzzy logic clutter filter as described by Dufton and
43 Collier (2015). In addition to these corrections, a correction for partial beam blocking and attenuation (A_H) have also been
44 applied. From this corrected Z_H , rainfall rate was retrieved using the Marshall-Palmer relation ($R(Z)=aZ^b$, with $a=200$ and
45 $b=1.6$ as is used by the UK Met Office) to derive rain rate for their operational network of C-band radars (Marshall and
46 Palmer, 1948). For access to the observations made with the NXPOL during COPE, please see the Centre for Environmental

47 Data Analysis (CEDA) archive for the campaign at [http://data.ceda.ac.uk/badc/microscope/data/ncas-mobile-xband-](http://data.ceda.ac.uk/badc/microscope/data/ncas-mobile-xband-radar/version-2/)
48 [radar/version-2/](http://data.ceda.ac.uk/badc/microscope/data/ncas-mobile-xband-radar/version-2/) (Blyth et al., 2013).

49

50 **Figure 5. Example of observations made by NXPoL (located at the centre black dot) at 0.5° elevation on 3 August 2013 at 1332**
51 **UTC showing: a) calibrated but unfiltered and uncorrected horizontal reflectivity (Shown as to display the importance and impact**
52 **of the data processing) , b) calibrated, filtered and corrected differential reflectivity, c) specific horizontal attenuation (A_H) and d)**
53 **rainfall rates derived using the Marshall-Palmer relation ($R(Z)=aZ^b$, with $a=200$ and $b=1.6$). The missing spokes of data in A_H are**
54 **caused by quality control settings in the processing routine that reject radials that do not meet certain thresholds. The sub-panel**
55 **in d) shows an expanded section of the line of intense rainfall ($>120\text{mm/hr}$ in some pixels; please note the expanded colorbar to the**
56 **top of the sub-panel) to the southeast of the radar. Range rings are drawn every 10km.**



57

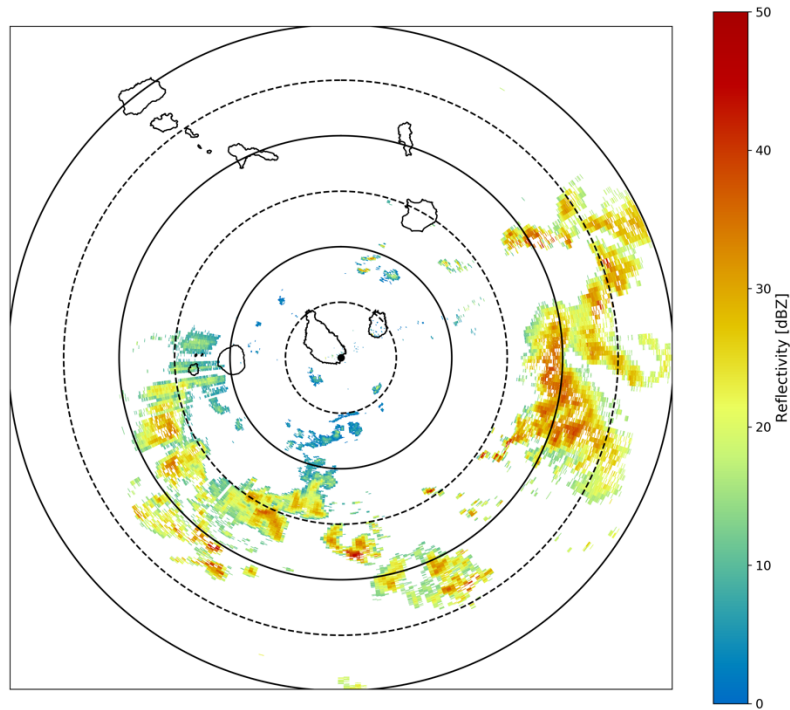
58 **3.2 ICE-D**

59 NXPoI was deployed at Praia, Cape Verde (14°55'N 23°31'W) during July and August 2015 in the UK's Ice in Clouds
60 Experiment-Dust (ICE-D). The goal of ICE-D was to determine how desert dust affects primary nucleation of ice particles in
61 convective and layer clouds and the subsequent development of precipitation and glaciation of the clouds. In addition to
62 NXPoI, the FAAM BAe-146 research aircraft and the University of Manchester ground-based aerosol laboratory were
63 deployed. All data from this campaign may be found on CEDA at
64 <http://catalogue.ceda.ac.uk/uuid/55b5d76a7edb42e39933c1edc37f7b90>.

65
66 The main objective of NXPoI was to provide the spatial and temporal distribution of the clouds, to identify suitable cloud
67 regions for the aircraft to sample and to provide coordinated observations of the development of precipitation within about
68 100 km of the island. Two modes of data collection were implemented dependent on the synoptic conditions and location of
69 cloud development. In "surveillance mode", NXPoI was configured to maximise its observable range. In this mode,
70 observations were made out to 300 km at several low elevations. An example surveillance mode PPI observed on 23 August
71 2015 using the surveillance mode is given in Figure 6. Use of the radar in this mode was found to be invaluable for near-term
72 mission planning and directing the use of the FAAM once it was airborne. For suitable clouds at closer range, NXPoI
73 operated in "data-collection mode", providing higher spatial and temporal resolution observations; volumes of 12 elevations
74 from 0.5 up to 12 degrees were collected out to a range of 150 km similar to COPE.

75
76

77 **Figure 6. Example of a surveillance mode PPI observed by NXPol at 2019UTC on 23 August 2015 while on the ICE-D deployment**
78 **in Praia, Cape Verde. Range rings are drawn every 50km. The thick black outlines are the islands of Cape Verde.**



79

80 **3.3 Radar Applications in Northern Scotland (RAINS)**

81 COPE and ICE-D are examples of the use of the NXPol for traditional IOP based operations. This section highlights the use
82 of the NXPol for semi-permanent operations. Previous studies have shown the value of operating a mobile polarimetric X-
83 band radar in coastal regions to fill gaps in the coverage of national operational radar networks (Matrosov et al. 2005).
84 Matrosov et al. (2005) found that the NOAA X-band radar (9.34 Hz, 30kW peak power) was effective in covering an area up
85 to 40–50 km in radius offshore adjacent to a region that is prone to flooding during wintertime land landfalling Pacific
86 storms. More recently, the Collaborative Adaptive Sensing of the Atmosphere (CASA) Engineering Research Center’s X-
87 band dual-polarisation radar network has shown the utility of short-range radars at making high-resolution observations of
88 rainfall that are close to the ground over a variety of conditions (Wang and Chandrasekar, 2010).

89

90 During the RAINS campaign, the NXPol was installed at Army Base 39 Engineer Regiment, Kinloss, northeast Scotland
91 from January 2016 to August 2016. This deployment was a joint project between NCAS, the Scottish Environment
92 Protection Agency (SEPA), the University of Leeds and the UK Met Office with the goal of examining the value of
93 additional and higher-resolution radar observations in this region for creating more accurate QPE and flood forecasts.
94 Beyond just improving radar coverage in Northern Scotland, the data collected from the NXPol is also being used to
95 examine the specific improvements in QPE that dual-polarisation observations can provide hydrological models in this
96 region, which is characterised by low melting levels (i.e. low bright bands) and mountainous terrain. In Figure 7 we show an
97 example of two differing QPEs during a typical precipitation event during the deployment. The observations and the two
98 rainfall rate retrievals are shown here to highlight the potential differences in rainfall rate methods that are being explored as
99 part of RAINS. In particular we highlight the difference between the rainfall rate calculated using the Marshall-Palmer
00 relation ($R(Z)=aZ^b$, with $a=200$ and $b=1.6$) which is used by the UK Met Office and rainfall rates calculated using the
01 $R(Z_H, K_{DP})$. The $R(Z_H, K_{DP})$ is described in Diederich et al. (2015b) and here we use $a = 16.9$ and $b = 0.801$. The entire
02 RAINS dataset may be requested from the author as it is still undergoing primary analysis with SEPA and has not been
03 released publically. Once this analysis has been concluded the dataset will be available on CEDA.

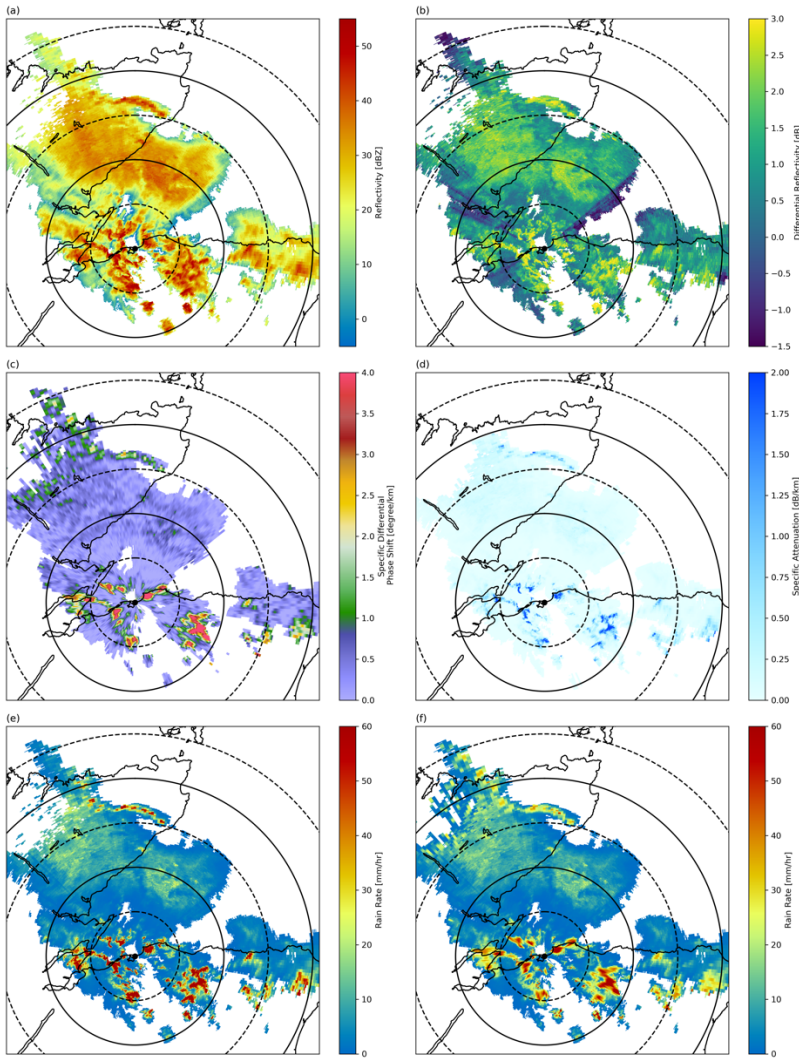
04

05 As part of the work in RAINS, a set of software tools was created to convert NXPol data into the Met Office NIMROD
06 format using a combination of gridding software (Py-ART or LROSE) and bespoke scripts developed by NCAS. Many UK
07 agencies (i.e. the Environment Agency and SEPA) use this format in their modelling and analysis tools such as HyRAD,
08 developed by the UK's Centre for Ecology and Hydrology (CEH). These scripts may be requested from the authors.

09

10

11 **Figure 7. Observations and derived rainfall rates from the RAINS campaign on 20 July 2016 at 0409 UTC at 1.5° elevation: NXPOL**
 12 **is located at the black dot and range rings are drawn every 25km. (a) calibrated, corrected and filtered Z_H classified as**
 13 **precipitation echoes; (b), (c) and (d) calibrated, corrected and filtered Z_{DR} , K_{DP} , and A_H , (e) rainfall rate calculated using the**
 14 **Marshall-Palmer relation ($R(Z)=aZ^b$, with $a=200$ and $b=1.6$) and (f) rainfall rates calculated using $R(Z_H, K_{DP})$. NXPOL is located at**
 15 **the black dot and range rings are drawn every 25km.**



16

19

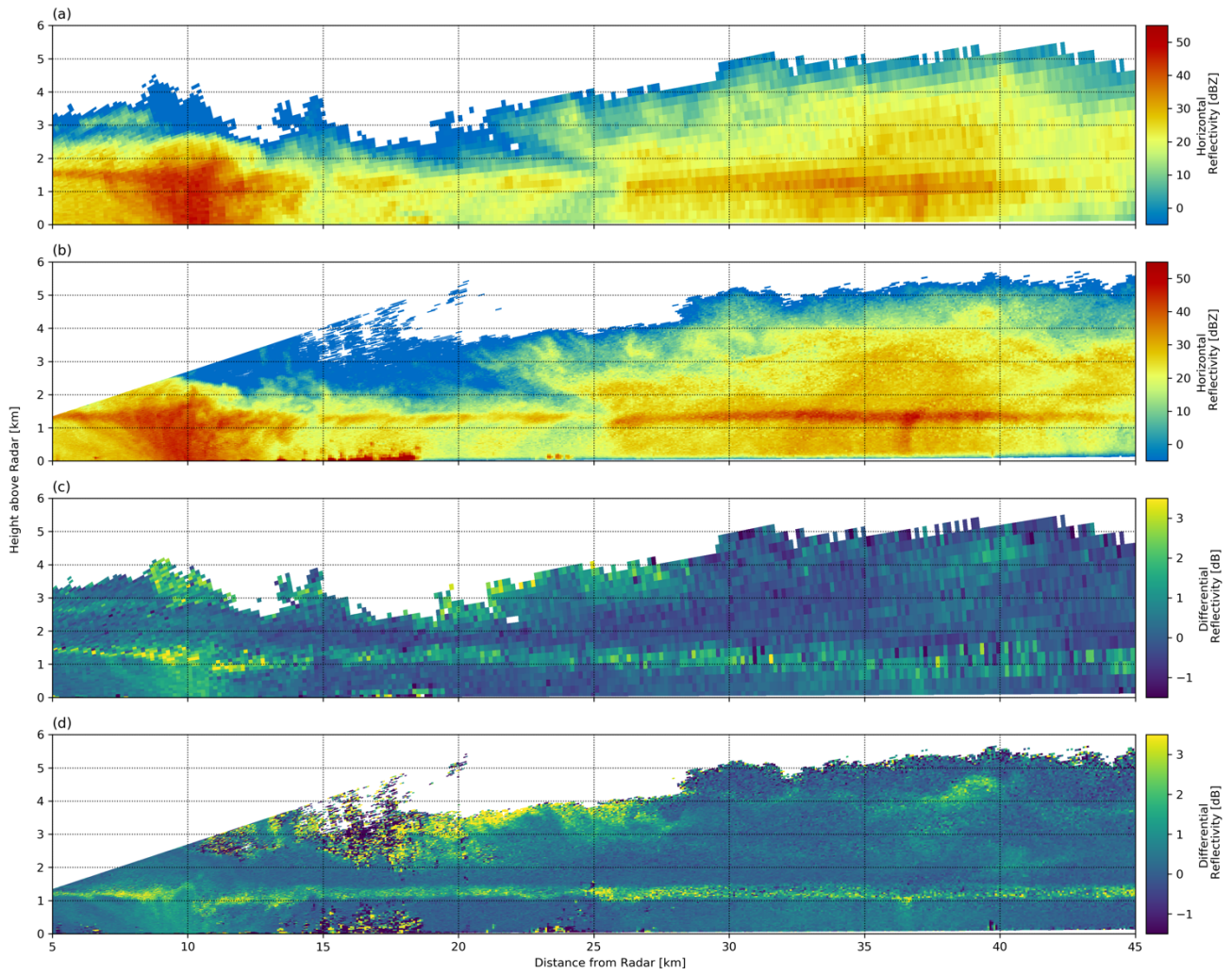
17 **4 Ongoing Work at NFARR**

18 In between major field deployments, the NXPoI makes continuous observations at the National Facility for Atmospheric
19 Radar Research (NFARR), located near Chilbolton in Hampshire, UK. This enables NXPoI to work in coordination with the
20 other state-of-the-art radar facilities located at the observatory to make novel observations of high impact wintertime storms
21 and summertime convective events using an array of ground-based remote sensing and in situ observations. The goal of this
22 work is to improve flood forecasting in the UK by using these novel observations to drive the development of physical
23 parameterisations in high-resolution numerical weather prediction models.

24
25 Most significantly, this work includes NXPoI making coincidental RHI scans of frontal events with the Chilbolton Advanced
26 Meteorological Radar (CAMRa), which is the largest steerable meteorological radar in the world. CAMRa operates at S-
27 band (~3 GHz), and its 25m antenna creates a beam width of only 0.25°. This results in the ability to make high-resolution
28 observations at far ranges (i.e. at 100 km from the dish, the resolution of a 0.25° beam is 0.4 km). Like the NXPoI, CAMRa
29 has dual-polarisation and Doppler capabilities. For a full description of CAMRa, please see Goddard et al. (1984). An
30 example of coincidental observations from CAMRa and the NXPoI on January 12th, 2017 at 13:36 UTC are shown in Figure
31 8. Currently, observations from both radars may be requested from the authors as they still undergoing its primary analysis.
32 The datasets will also become public on CEDA by 2020 after the 2 year embargo period for this campaign is over.

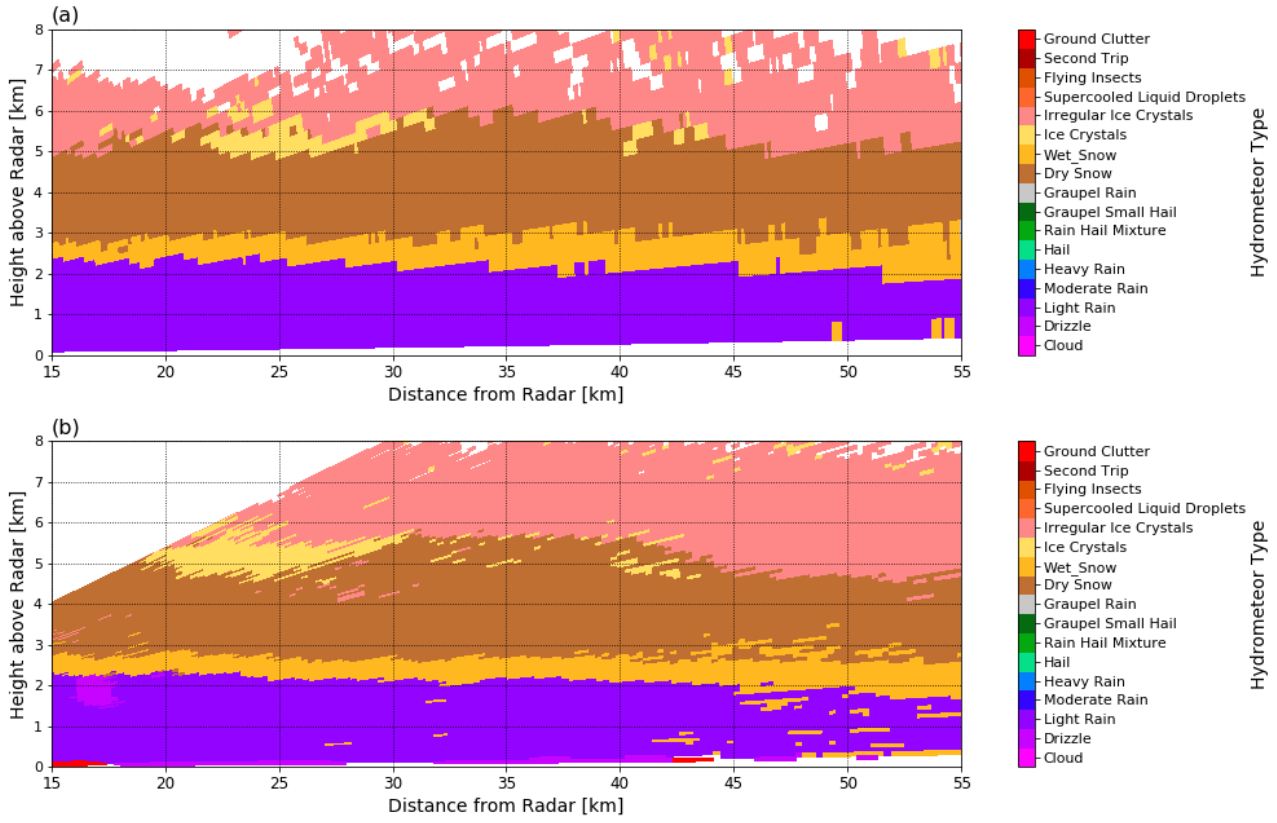
33
34 As part of the ongoing research with NXPoI, the use of hydrometeor classification algorithms (HCAs; also referred to as
35 particle identification or PID) to explore cloud microphysics is being pursued. Such an HCA has been initially implemented
36 for the NXPoI using the framework provided by LROSE (Dixon et al. 2012). The HCA is a fuzzy logic approach, and the
37 membership functions are based largely on the work of Dolan and Rutledge (2009) and Thompson et al. (2014). An
38 example result of the HCA applied to NXPoI and CAMRa observations from May 17th, 2017 at 12:24 UTC is shown in
39 Figure 9. The NXPoI's HCA results are part of on-going research and have not yet been fully validated. As such, Figure 9 is
40 shown only to demonstrate the type of on-going investigations enabled by the NXPoI's observations. Nevertheless, the
41 comparison shows good qualitative agreement between the algorithms applied to the two radars. Future work will include
42 validation with in situ observations made with FAAM. We hope that the use of multiple frequencies will help constrain and
43 reduce uncertainty associated scattering parameters within the retrieval.

44 **Figure 8. Coincident RHIs of Z_H (a and b) and Z_{DR} (c and d) from the NXPol (a and c) and CAMRa (b and d) on 12 January 2017**
45 **at 13:36 UTC.**



46

Figure 9. Coincident RHIs from the NXPoI (a) and CAMRa (b) on 17 May 2017 at 12:24 UTC with the HCA applied to both.



49 **5 Summary**

50 Here we have summarised the key technical characteristics of the NXPoI and the infrastructure used to deploy the system
51 autonomously at remote locations. We have also shown examples of its successful use in four differing scientific campaigns.
52 As is shown in the examples, the NXPoI is a highly capable and flexible instrument for use in examining the microphysics of
53 clouds and producing QPE. As described in Section 4, in between bespoke deployments to remote locations, the NXPoI will
54 be located at NFARR to make continuous observations in conjunction with other instruments at this site. The NCAS and
55 Leeds University Radar Group welcomes any collaborations that utilise the NXPoI and its observations.

56

57 For further information on the use of the NXPoI including instrument access policies, data format, NXPoI specific analysis
58 software and availability, please see the NXPoI instrument homepage at: [https://www.ncas.ac.uk/index.php/en/about-](https://www.ncas.ac.uk/index.php/en/about-amf/263-amf-main-category/amf-x-band-radar/1098-x-band-radar-overview)
59 [amf/263-amf-main-category/amf-x-band-radar/1098-x-band-radar-overview](https://www.ncas.ac.uk/index.php/en/about-amf/263-amf-main-category/amf-x-band-radar/1098-x-band-radar-overview).

60

61 **Acknowledgements.**

62 Numerous people have provided assistance in the development and deployment of the NXPoI since its purchase in 2012. We
63 thank them for their contributions and support in this effort. In particular, we thank Selex ES GmbH for their excellent
64 support and Mike Dixon of NCAR's Earth Observing Laboratory for his continued help in adapting LROSE to the needs of
65 the NXPoI. The lead author would like to acknowledge the "Shut Up and Write" group in the School of Earth and
66 Environment at the University of Leeds. Without the weekly space, time, and support this group offers, this manuscript
67 would not have been written.

68 **References**

- 69 Ahlbom, A., Bergqvist, U., Bernhardt, J. H., Cesarini, J. P., Court, L. A., Grandolfo, M., Hietanen, M., McKinlay, A. F.,
70 Repacholi, M. H., Sliney, D. H., Stolwijk, J. A. J., Swicord, M. L., Szabo, L. D., Taki, M., Tenforde, T. S., Jammet, H. P.
71 and Matthes, R.: Guidelines for limiting exposure to time-varying electric, magnetic, and electromagnetic fields (up to 300
72 GHz), *Health physics.*, 74(4), 494–521, 1998.
- 73
- 74 Antonini, A., Melani, S., Corongiu, M., Romanelli, S., Mazza, A., Ortolani, A. and Gozzini, B.: On the Implementation of a
75 Regional X-Band Weather Radar Network, *Atmosphere*, 8(2), 25–20, doi:10.3390/atmos8020025, 2017.
- 76
- 77 Biggerstaff, M. I. and Co-Authors: The shared mobile atmospheric research and teaching radar: A collaboration to enhance
78 research and teaching. *Bulletin of the American Meteorological Society*, 86(9), 1263–1274. [https://doi.org/10.1175/BAMS-](https://doi.org/10.1175/BAMS-86-9-1263)
79 86-9-1263, 2005.
- 80
- 81 Bluestein, H. B., French, M. M., Tanamachi, R. L., Frasier, S., Hardwick, K., Junyent, F. and Pazmany, A. L.: Close-Range
82 Observations of Tornadoes in Supercells Made with a Dual-Polarization, X-Band, Mobile Doppler Radar, *Mon. Wea. Rev.*,
83 135(4), 1522–1543, doi:10.1175/MWR3349.1, 2007.
- 84
- 85 Bluestein, H. B. and Co-Authors.: Radar in Atmospheric Sciences and Related Research: Current Systems, Emerging
86 Technology, and Future Needs, *Bulletin of the American Meteorological Society*, 95(12), 1850–1861, doi:10.1175/bams-d-
87 13-00079.1, 2014.
- 88
- 89 Blyth, A. M., Benestad, R. E., Krehbiel, P. R. and Latham, J.: Observations of Supercooled Raindrops in New Mexico
90 Summertime Cumuli, *J. Atmos. Sci.*, 54(4), 569–575, doi:10.1175/1520-0469(1997)054<0569:oosrin>2.0.co;2, 1997.
- 91
- 92 Blyth, A., Bennett, L., Choularton, T. W., Illingworth, A. J. and Norton, E. G.: MICROphysicS of CONvective PrEcipitation
93 (MICROSCOPE) project: In-situ airborne atmospheric and ground-based radar measurements, [online] Available from:
94 <http://catalogue.ceda.ac.uk/uuid/8440933238f72f27762005c33d2aa278>, October 2, 2017.

95 Blyth, A. M., Bennett, L. J. and Collier, C. G.: High-resolution observations of precipitation from cumulonimbus clouds,
96 Met. Apps, 22(1), 75–89, doi:10.1002/met.1492, 2015.

97

98 Borgmann, J., Hannesen, R., Göltz, P. and Gekat, F.: Development and Application of a Polarimetric X-Band Radar for
99 Mobile and Stationary Applications, 33rd Conference on Radar Meteorology, American Meteorological Society, Cairns,
00 Queensland, Australia. 2007.

01

02 Bringi, V. N. and Chandrasekar, V.: Polarimetric Doppler Weather Radar, Cambridge University Press, Cambridge. 2001.

03

04 Bringi, V., Zahrai, A., Zrníc, D., Doviak, R. J., Bringi, V., Ryzhkov, A. and Zrníc, D.: Considerations for Polarimetric
05 Upgrades to Operational WSR-88D Radars, 17(3), 257–278, doi:10.1175/1520-0426(2000)017<0257:CFPUTO>2.0.CO;2,
06 2000.

07

08 Chandrasekar, V. and Bharadwaj, N.: Orthogonal Channel Coding for Simultaneous Co- and Cross-Polarization
09 Measurements, J. Atmos. Oceanic Technol., 26(1), 45–56, doi:10.1175/2008JTECHA1101.1, 2009.

10

11 Diederich, M., Ryzhkov, A., Simmer, C., Zhang, P. and Trömel, S.: Use of Specific Attenuation for Rainfall Measurement at
12 X-Band Radar Wavelengths. Part I: Radar Calibration and Partial Beam Blockage Estimation, J. Hydrometeor, 16(2), 487–
13 502, doi:10.1175/JHM-D-14-0066.1, 2015a.

14

15 Diederich, M., Ryzhkov, A., Simmer, C., Zhang, P. and Trömel, S.: Use of Specific Attenuation for Rainfall Measurement at
16 X-Band Radar Wavelengths. Part II: Rainfall Estimates and Comparison with Rain Gauges, J. Hydrometeor, 16(2), 503–516,
17 doi:10.1175/JHM-D-14-0067.1, 2015b.

18

19

20 Dixon, M., Lee, W.-C., Daniels, M., Martin, C., Cohn, S. and Brown, B.: Community Software Tools for the Radars, Lidars
21 and Profilers of the NSF Lower Atmosphere Observing Facilities. [online] Available from:
22 <https://www.eol.ucar.edu/system/files/RadarSoftwareRequestForComment.20120918.pdf>, 2012.

23 Dixon, M., W.-C. Lee, B. Rilling, and C. Burghart: CfRadial data file format: Proposed CF-compliant netCDF format for
24 moments data for RADAR and LIDAR in radial coordinates. NCAR, 66 pp. [Available online at
25 [www.eol.ucar.edu/system/files /CfRadialDoc.v1.3.20130701.pdf](http://www.eol.ucar.edu/system/files/CfRadialDoc.v1.3.20130701.pdf)], 2013
26
27 Dolan, B. and Rutledge, S. A.: A Theory-Based Hydrometeor Identification Algorithm for X-Band Polarimetric Radars,
28 *Journal of Atmospheric and Oceanic Technology*, 26(10), 2071–2088, doi:10.1175/2009JTECHA1208.1, 2009.
29
30 Dufton, D. R. L. and Collier, C. G.: Fuzzy logic filtering of radar reflectivity to remove non-meteorological echoes using
31 dual polarization radar moments, *Atmos. Meas. Tech.*, 8(10), 3985–4000, doi:10.5194/amt-8-3985-2015, 2015.
32
33 Fabry, F.: *Radar Meteorology: Principles and Practice*, Cambridge University Press, Cambridge, UK, 2015.
34
35 Forget, P., Saillard, M., Guérin, C. A., Testud, J. and Le Bouar, E.: On the Use of X-Band Weather Radar for Wind Field
36 Retrieval in Coastal Zone, *J. Atmos. Oceanic Technol.*, 33(5), 899–917, doi:10.1175/JTECH-D-15-0206.1, 2016.
37
38 Galletti, M., Chandra, M. and Borner, T.: Degree of polarization for weather radars, *IEEE International Geoscience and*
39 *Remote Sensing Symposium*, Barcelona, Spain, 2007.
40
41 Galletti, M. and Zmic, D. S.: Degree of Polarization at Simultaneous Transmit: Theoretical Aspects, *IEEE Geosci. Remote*
42 *Sensing Lett.*, 9(3), 383–387, doi:10.1109/LGRS.2011.2170150, 2012.
43
44 Geerts, B., and Coauthors: The 2015 Plains Elevated Convection At Night (PECAN) field project. *Bulletin of the American*
45 *Meteorological Society*, BAMS-D-15-00257.1. <https://doi.org/10.1175/BAMS-D-15-00257.1>, 2016.
46
47 Goddard, J.W.F., Eastment, J.D. and Thurai, M.: 'The Chilbolton Advanced Meteorological Radar: a tool for
48 multidisciplinary atmospheric research', *Electronics & Communication Engineering Journal*, 1994, 6, 77-86. DOI:
49 10.1049/ecej:19940205
50

51 Golding, B., Clark, P. and May, B. (2005), The Boscastle flood: Meteorological analysis of the conditions leading to
52 flooding on 16 August 2004. *Weather*, 60: 230–235. doi:10.1256/wea.71.05
53

54 Heistermann, M., Jacobi, S. and Pfaff, T.: Technical Note: An open source library for processing weather radar data
55 (*wradlib*), *Hydrology and Earth System Sciences*, 17(2), 863–871, doi:10.5194/hess-17-863-2013, 2013.
56

57 Heistermann, M., Collis, S., Dixon, M. J., Giangrande, S., Helmus, J. J., Kelley, B., Koistinen, J., Michelson, D. B., Peura,
58 M., Pfaff, T. and Wolff, D. B.: The Emergence of Open-Source Software for the Weather Radar Community, *Bulletin of the*
59 *American Meteorological Society*, 96(1), 117–128, doi:10.1175/BAMS-D-13-00240.1, 2015.
60

61 Helmus, J. J. and Collis, S. M., (2016). The Python ARM Radar Toolkit (Py-ART), a Library for Working with Weather
62 Radar Data in the Python Programming Language. *Journal of Open Research Software*. 4(1), p.e25. doi:
63 <http://doi.org/10.5334/jors.119>.
64

65 Jameson, A. R., Murphy, M. J. and Krider, E. P.: Multiple-Parameter Radar Observations of Isolated Florida Thunderstorms
66 during the Onset of Electrification, *Journal of Applied Meteorology*, 35(3), 343–354, doi:10.1175/1520-
67 0450(1996)035<0343:mprooi>2.0.co;2, 1996.
68

69 Kato, A. and Maki, M.: Localized Heavy Rainfall Near Zoshigaya, Tokyo, Japan on 5 August 2008 Observed by X-band
70 Polarimetric Radar—Preliminary Analysis—, *SOLA*, doi:10.2151/sola.2009–023, 2009.
71

72 Kumjian, M.: Principles and applications of dual-polarization weather radar. Part I: Description of the polarimetric radar
73 variables, *J. Operational Meteor.*, 1(19), 226–242, doi:10.15191/nwajom.2013.0119, 2013a.
74

75 Kumjian, M.: Principles and applications of dual-polarization weather radar. Part II: Warm- and cold-season applications, *J.*
76 *Operational Meteor.*, 1(20), 243–264, doi:10.15191/nwajom.2013.0120, 2013b.
77

78 Kumjian, M.: Principles and applications of dual-polarization weather radar. Part III: Artifacts, *J. Operational Meteor.*, 1(21),
79 265–274, doi:10.15191/nwajom.2013.0121, 2013c.

80

81 Kumjian, M. R. and Ryzhkov, A. V.: The Impact of Size Sorting on the Polarimetric Radar Variables, *Journal of*
82 *Atmospheric Sciences*, 69(6), 2042–2060, doi:10.1175/JAS-D-11-0125.1, 2012.

83

84 Leon, D. C., and Coauthors: The CONvective Precipitation Experiment (COPE): Investigating the origins of heavy
85 precipitation in the southwestern UK. *Bulletin of the American Meteorological Society*, 150908092010003–
86 150908092010052, doi:10.1175/BAMS-D-14-00157.1, 2015.

87

88 Maki, M., Iwanami, K., Misumi, R., Park, S.-G., Moriwaki, H., Maruyama, K.-I., Watabe, I., Lee, D.-I., Jang, M., Kim, H.-
89 K., Bringi, V. N. and Uyeda, H.: Semi-operational rainfall observations with X-band multi-parameter radar, edited by A.
90 Seed and G. Austin, *Atmos. Sci. Lett.*, 6(1), 12–18, doi:10.1002/asl.84, 2005.

91

92 Marshall, J. S. and Palmer, W.: The Distribution of Raindrops with Size, *Journal of Meteorology*, 1948.

93

94 Matrosov, S. Y., D. E. Kingsmill, B. E. Martner, and F. M. Ralph, 2005: The utility of X-band polarimetric radar for
95 quantitative estimates of rainfall parameters. *J. Hydrometeor*, 6, 248–262.

96

97 Mishra, K. V., Krajewski, W. F., Goska, R., Ceynar, D., Seo, B.-C., Kruger, A., Niemeier, J. J., Galvez, M. B., Thurai, M.,
98 Bringi, V. N., Tolstoy, L., Kucera, P. A., Petersen, W. A., Grazioli, J. and Pazmany, A. L.: Deployment and Performance
99 Analyses of High-Resolution Iowa XPOL Radar System during the NASA IFloodS Campaign, *J. Hydrometeor*, 17(2), 455–
00 479, doi:10.1175/JHM-D-15-0029.1, 2016.

01

02 Pazmany, A. L., Mead, J. B., Bluestein, H. B., Snyder, J. C., & Houser, J. B. (2013). A mobile rapid-scanning X-band
03 polarimetric (RaXPOL) doppler radar system. *Journal of Atmospheric and Oceanic Technology*, 30(7), 1398–1413.
04 <https://doi.org/10.1175/JTECH-D-12-00166.1>

05

06 Thompson, E. J., Rutledge, S. A., Dolan, B., Chandrasekar, V. and Cheong, B. L.: A Dual-Polarization Radar Hydrometeor
07 Classification Algorithm for Winter Precipitation, *J. Atmos. Oceanic Technol.*, 31(7), 1457–1481, doi:10.1175/JTECH-D-
08 13-00119.1, 2014.

09

10 Wang, Y. and Chandrasekar, V.: Quantitative Precipitation Estimation in the CASA X-band Dual-Polarization Radar
11 Network, *J. Atmos. Oceanic Technol.*, 27(10), 1665–1676, doi:10.1175/2010JTECHA1419.1, 2010.

12

13 Wurman, J., Straka, J., Rasmussen, E., Randall, M. and Zahrai, A.: Design and deployment of a portable, pencil-beam,
14 pulsed, 3-cm Doppler radar, *Journal of Atmospheric and Oceanic Technology*, 14, 1502–1512, doi:10.1175/1520-
15 0426(1997)014<1502:DADOAP>2.0.CO;2, 1997.

16

17 Wurman, J., Dowell, D., Richardson, Y., Markowski, P., Rasmussen, E., Burgess, D., Wicker, L. and Bluestein, H. B.: The
18 Second Verification of the Origins of Rotation in Tornadoes Experiment: VORTEX2, *Bulletin of the American
19 Meteorological Society*, 93(8), 1147–1170, doi:10.1175/BAMS-D-11-00010.1, 2012.

20

21 Yanting Wang and Chandrasekar, V.: Polarization isolation requirements for linear dual-polarization weather Radar in
22 simultaneous transmission mode of operation, *IEEE Trans. Geosci. Remote Sensing*, 44(8), 2019–2028,
23 doi:10.1109/tgrs.2006.872138, 2006.